International Journal of Engineering

Journal Homepage: www.ije.ir

A New Approach for Determination of Neck-Pore Size Distribution of Porous Membranes via Bubble Point Data

M. Arjmandi*[a], O. Pirouzram[b], A. Ahmadpour[a]

[a] *Department of Chemical Engineering, Faculty of Engineering, Ferdowsi University of Mashhad, Mashhad, Iran*
[b] *Department of Chemical Engineering, Faculty of Engineering, Kurdistan University, Kurdistan, Iran*

PAPER INFO

Paper history:
Received 19 July 2014
Received in revised form 12 March 2014
Accepted 30 April 2015

Keywords:
Membrane
NPSD
Regularization
Cross-Validation

ABSTRACT

Reliable estimation of the porous membranes neck-pore size distribution (NPSD) is the key element in the design and operation of all membrane separation processes. In this paper, a new approach is presented for reliable determination of NPSD of porous membranes using wet flow-state bubble point test data. For this purpose, a robust method based on the linear regularization theory is developed to extract NPSD of membranes from bubble point test data. The performance of the proposed method is tested using various experimental data. The predicted results clearly demonstrate that the proposed method can successfully predict the proper NPSD from a set of bubble point test data.

doi: *10.5829/idosi.ije.2015.28.06c.01*

1. INTRODUCTION

Porous ceramic, metal and polymer films are widely used as filter or membrane in various separation processes. They are used in different applications such as materials supporting, noise suppressor, biomedical implants, gas dispersers, distillation and centrifugation. The membrane technology is also having wide applications in water and wastewater industry, food industry, pharmaceutical and medical industry, biotechnology, air filtration and gas purification. Characterization of membranes structure in terms of pore size distribution (PSD) is an important step in research and development of porous materials [1-3]. The PSD is a useful parameter for optimization of different membrane processes and commercial manufacturing of the membranes. Various methods have been proposed for characterization of PSD of porous membranes. The major ones are presented below: Bubble pressure breakthrough method is based on the measurement of the pressure necessary to blow air through a porous membrane filled with liquid [4-6]. Mercury porosimetry is based on the same principles as the bubble pressure method; but now a non-wetting (mercury) is used to fill a dry membrane [7, 8]. Electron microscopy which is available to view the top or cross sections of membranes, such as scanning electron microscopy (SEM) [9], transmission electron microscopy (TEM) [10] etc... Atomic force microscopy used to study of non-conducting materials surface (down to the scale of nanometers) [11, 12]. Solute retention challenge, in which pore sizes can be evaluated by measurement of rejection for various solutes of increasing molecular weights or hydrodynamic sizes [13]. Adsorption–desorption methods, in which pore size distribution can be also analized by gas adsorption/desorption devices (BET adsorption theory is one of these methods) [14]. Thermoporometry is based on the fact that the solidification point of the vapour condensed in the pores is a function of the interface curvature [15, 16]. Permporometry is based on the controlled blocking of pores by condensation of vapour and measurement of the gas flux through the membrane [17, 18]. NMR measurements method is determination of pore size in water-saturated membranes using nuclear magnetic resonance (NMR) [19, 20].

*Corresponding Author's Email: *mehrzad.arjmandi89@gmail.com* (M. Arjmandi)

Please cite this article as: M. Arjmandi, O. Pirouzram, A. Ahmadpour, A New Approach for Determination of Neck-Pore Size Distribution of Porous Membranes via Bubble Point Data, International Journal of Engineering (IJE), TRANSACTIONS C: Aspects Vol. 28, No. 6, (June 2015) 823-831

Some of those techniques such as liquid and gas flux measurements, solute retention test, liquid displacement method, permporometry etc... are useful to characterize the thin layer in asymmetric membranes but they don't give any insight into the structure of remaining membrane. However, the other methods such as gas adsorption–desorption, atomic force microscopy (AFM), mercury porosimetry, electron microscopy, thermoporometry etc... give complete information on the porous structure. Among various techniques available to predict the PSD of membranes, some of them operate according to the capillary flow and are called capillary flow porometery (CFP) [21]. The CFP method can be used for accurate measurement of the neck-pore size distribution (NPSD) of membranes with understanding wet and dry flow-state data and the flux of porometer fluid coming out of the pore which its size equals to r (G(r)). The CFP is a simple, non-destructive and rapid technique. In this study, a new method based on the linear regularization theory is developed to extract the NPSD of membranes from bubble point test data with using the minimum number of experimental and physical data (with only wet-flow state and without the need to G(r) function). The performance of the proposed method is also tested using different experimental data.

2. THEORY

2. 1. Bubble Point Method When a liquid is dropped on a solid surface, the result will be a surface tension between the gas- liquid, liquid-solid and gas-solid phases. That is why the porous screen is able to separate the two phases due to the capillary force. According to Equation (1), the surface tensions results in a contact angle. The contact angle is the angle conventionally measured through the liquid, where a liquid/vapor interface meets a solid surface.

$$Cos\theta = \frac{\sigma_{g-s} - \sigma_{1-s}}{\sigma_{g-1}} \quad (1)$$

where, σ is the surface tension; s, l and g are solid, liquid and gas/vapor phases, respectively. When $\sigma_{g-s} > \sigma_{1-s}$ and $\theta < 90^\circ$, the liquid wet the surface; while $\sigma_{g-s} < \sigma_{1-s}$ and $\theta > 90^\circ$ the liquid could not wet the solid surface. As it is shown in Figure 1, in the bubble point method, the membrane is placed in a chamber and a liquid is added above its surface. Water is usually used for hydrophilic membranes, while alcohols can be used for hydrophobic membranes. Then, the gas pressure is applied on the bottom surface of the membrane and gradually increases over time. During this process, the membrane pores are filled with the liquid and then membrane is cleaned with the help of gas bubbles blown from the bottom. Different steps of pore opening are shown in Figure 2. With increasing gas pressure, the liquid will be under pressure. When the pressure is high enough, the pressure force will overcome capillary force and the pores will be open quickly. The pore shape is irregular in most cases. However, with simple approximation, we assume a cylindrical shape of the pores with equivalent radius *r*. Several more sophisticated characterization methods related to the bubble point measurements have been also proposed. All of them use the Young-Laplace equation [22], which gives the pressure needed to displace one fluid by another through a pore with radius *r* as:

$$r = \frac{2\sigma\cos\theta}{P} \quad (2)$$

where, σ is the surface tension of liquid; θ is the contact angle of the liquid on the pore wall; and P is gas critical pressure required to reopen the pores (bubble point pressure). As shown in Figure 2, since the pressure p is related to the bubble point pressure and is also the highest pressure required to overcome the capillary forces, Equation (2) will represent the size of the pore neck. If the wetting is perfect ($\theta \approx 0$), we can also use the Cantor equation (Equation (3)).

$$r = \frac{2\sigma}{P} \quad (3)$$

According to Equations (2) and (3), if the gas pressure increases, pores with smaller radius will be opened. In other words, the larger pores are opened before the smaller ones. Opening of new pores can be studied by changing the flux of gas passing through the membrane. According to the dry and wet-state pressure-gas flux curve, we can obtain the distribution of the pore size in the membrane.

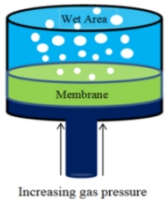

Figure 1. Schematic of bubble point method

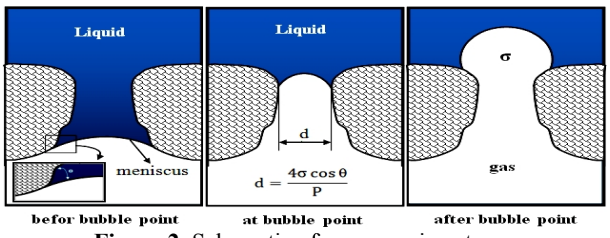

Figure 2. Schematic of pore opening steps.

In this study, we assume a system shown in Figure 3 to obtain data from a bubble point method. According to this figure, the membrane is placed between fluids A and B, and then pressure applies on the fluid A. When Δp increases from zero to the critical pressure P_0 (initial pressure for permeation), fluid A seeps through the membrane into the fluid B and the flux is measured with a flow meter. It is essential to note that the fluids A and B are immiscible. With further pressure increase on side A, more membrane pores will be opened and consequently the flux of A will be increased.

2. 2. Governing Equations The energy balance equation between two points marked on Figure 3 (1 and 2) is applied. It is important to note that the permeation of substance A through the membrane is very slow and the friction factor can be neglected in the energy equation. Therefore, instead of applying the total energy balance equation, the Bernoulli's equation can be written between the two points:

$$\frac{\Delta u_i^2}{2} + g\Delta Z + \frac{\Delta P}{\rho} \tag{4}$$

where, Δu_i is the velocity difference between points 1 and 2. According to Figure 3 and assuming that the fluid velocity is zero within the membrane, we have $\Delta u_i = u_i$. Also, the potential energy difference between two the sections is equal to ΔZ which can be considered zero. Finally, Equation (4) can be written as:

$$u_i = \sqrt{\frac{2P_i}{\rho}} \tag{5}$$

where, ρ is the density of fluid A. Flux of fluid A permeating through a square shaped membrane with pore radius r_i is equal to $Q(r_i)$ under pressure p_i:

$$Q(r_i) = \pi r_i^2 u_i f(r_i) dr_i \tag{6}$$

where, $f(r_i)dr_i$ is the number of pores with radius r_i in unit surface of the membrane. Also, according to Equation (6), it is assumed that the membrane pores, regardless of the pores shape, have a circular cross section area (Figure 4). By inserting Equation (5) into Equation (6) and rewriting, it gives:

$$Q(r_i) = \pi r_i^2 \sqrt{\frac{2P_i}{\rho}} f(r_i) dr_i \tag{7}$$

Then, by inserting Equation (3) into Equation (7) we will have:

$$Q(r_i) = \pi \sqrt{4 r_i \sigma_{A-B} \cos\theta} f(r_i) dr_i \tag{8}$$

Finally, Equation (8) can be written as:

$$Q(r_i) = G(r_i) f(r_i) dr_i \tag{9}$$

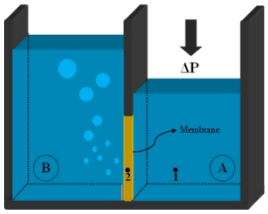

Figure 3. Schematic of the system used in this study for derived governing equations.

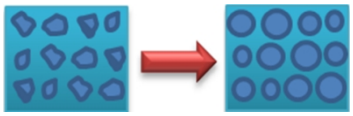

Figure 4. Schematic of cross section area of pores

where:

$$Q(r_i) = \pi \sqrt{4 r_i \sigma_{A-B} \cos\theta} \tag{10}$$

In addition, under pressure P_i, the total flux of gas passing through the membrane is equal to:

$$Q_t = \sum_{n=0}^{i} Q_n = \sum_{n=0}^{i} Q(r_n) = \int dQ_n = \int_{r_{\min}}^{r_{\max}} G(r) f(r) dr \tag{11}$$

The equation above provides the total flux of fluid passing through the membrane and also states that the total flux depends on the pore size, pore size distribution and other parameters (pore radius, surface tension, and contact angle) shown by $G(r)$. In other words, function $G(r)$ presents flux of fluid A passing through the pore with radius equal to r. Additionally, Equation (11) is general and comprehensive equation that all parameters except $G(r_i)$ for a certain membrane are known. Function $G(r)$ depends on various conditions and the way of calculating flux of fluid through pore with radius r. In this study, we intended to obtain neck-pore size distribution regardless of the tortuosity and thickness of the membrane. For this reason, the function $G(r_i)$ is defined by Equation (10). PiaÎtkiewicz et al. [23], considered the tortuosity and thickness of the membrane and used Hagen-Poiseuille equation for the function $G(r_i)$ as follows:

$$G(r_i) = \frac{\pi \Delta \mathrm{Pr}_i^4}{8 L \mu \tau} \tag{12}$$

where, μ is viscosity of fluid A; L is the thickness of the membrane; and τ is the tortuosity factor.

Treating expression (11) as an integral equation, using Equation (2) in a general form for change of variables, differentiating it with respect to P and solving for function $f(r)$ results in the following expression for relative pore size distribution function f [23]:

$$f(r) = ((\frac{8\pi}{\mu L \tau})(\gamma \cos\theta)^5)^{-1}(\frac{dQ}{dP} - \frac{Q}{P})(P)^5 \quad (13)$$

There are two numerical problems in using Equation (13). First, for a wet flow state bubble point test, if $P > P_{\max}$ and $P < P_{\max}$ both $(\frac{dQ}{dP})$ and $(\frac{Q}{P})$ are equal and $(\frac{dQ}{dP} - \frac{Q}{P}) = 0$. Therefore, at these pressure ranges the distribution function, $f(r)$, is zero (from Equation (13)). The second numerical problem encountered using Equation (13) for determination of PSD results a smooth curve through the data $(\frac{dQ}{dP} = \frac{P}{Q})$. Nowadays, these problems have been treated, but according to the basic computational (Equation (13)) the $G(r)$ function is always required.

Also, the measured ratio of flow rates through wet (Q) and dry sample (Q_d) can be used for obtaining the flow-based pore-neck size distribution $f(r)$ as [21]:

$$\frac{Q}{Q_d} = \int_{r_{\min}}^{r_{\max}} f(r)dr \quad (14)$$

The PSD measured by Equation (14) are not expected to be affected either by tortuosity or by thickness of the membrane ($G(r)$). According to above equation, the dry run plot obtained without wetting the membrane was used as the references. However, this equation is much simpler than the Equation (13) to prediction of PSD. Also, the investigations have shown that the tortuosity and the thickness of the membranes did not affect the value of pore-neck diameter determined through the CFP [21]. The following procedure for solving Equation (11) does not need to know the function $G(r)$ and dry flow-state data (Q_d).

2. 3. Solving Method Equation (11) which is a general equation providing the membrane pore size distribution is known as Fredholm integral equation. General linear integral equation is written as [24-26]:

$$f(x)h(x) + \int_{\alpha(x)}^{\beta(x)} K(x,y)f(y)dy = g(x) \quad (15)$$

Assuming α(x) = a, β(x) = b, and when h(x) = 0, then the Fredholm integral equation is the first kind equation. If $h(x) \neq 0$ and $a \le x \le b$, then the Fredholm integral equation is the second kind equation. If $g(x) = 0$, then the equation will be homogeneous. Thus, according to Equation (11), it is clear that the form of the equation is similar to the homogeneous first kind Fredholm integral equation [27]. Moreover, this equation has been used to calculate pore size distribution and energy distribution of the pores in the adsorption process. As noted above, Equation (11) helps to calculate the pore size distribution. One of the major problems is the lack of a suitable function for $G(r)$. In spite of using Equations (8) and (12), we still cannot comment specifically about the superiority of one over another, because we cannot verify the accuracy of the selected $G(r)$ function. Therefore, the results of these methods are not very reliable. Recently, Shahsavand and Niknam [28], provided a method (SHN1) that does not need to know the function $G(r)$. They have estimated the adsorbent pore size distribution by using the adsorption data of the heterogeneous adsorbent and the Kelvin equation. By this method, the Equation (11) will be written as follows (Equation (16)):

$$Q_t = \int_0^{r_k(p_i)} f(r)dr \quad (16)$$

The above equation can be written for discrete data as follows:

$$Q_t = \sum_{j=1}^{\sum_{k=1}^{i} M(P_k)} f(r) \times (\frac{r_{j+1} - r_{j-1}}{2}); \quad \text{j=1,2,…,N} \quad (17)$$

The matrix form of Equation (17) is $R.\underline{f} = \underline{Q}$. The solution of this equation will be $\underline{f} = R^{-1}.\underline{Q}$ where the inverse matrix is R^{-1}. The linear system of equations is generally solved by the method of least square. By minimizing the norm of the above equation matrix $(\min \left\| R\underline{f} - \underline{Q} \right\|^2)$, a linear equation of the following form is obtained [29].

$$(R^T R)\underline{f} = R^T \underline{Q} \quad (18)$$

Number of rows in matrix R is related to the number of experimental data (N) and number of columns is equal to multiplication N by number of discretization in each interval $(M(P)(N \times M(P))$. Since number of columns of matrix R is much greater than number of rows, the direct solution of the equation provides several results. Also, matrix R is an ill-posed one and it is not easy to inverse that. In such problems, using only the least square method is not a reliable and accurate criterion to find a response. These issues need more advanced techniques such as linear regularization and singular value decomposition (SVD) approach [30-34]. Thus, by using regularization, we will be able to write the above equation as follows:

$$(R^T R + \lambda B^T B)\underline{f} = R^T \underline{Q} \quad (19)$$

This method is known as Tikhonov regularization [35-37]. For the first order regularization, the double band B matrix has one fewer rows than its columns.

$$B=\begin{bmatrix} -1 & 1 & 0 & 0 & 0 \\ 0 & -1 & 1 & 0 & 0 \\ . & . & . & . & . \\ . & . & . & . & . \\ 0 & 0 & 0 & -1 & 1 \end{bmatrix} \quad (20)$$

Similarly, as shown in Equations (21) and (22), the B matrix has two or three rows fewer than their columns when second or third orders of regularization are employed.

$$B=\begin{bmatrix} -1 & 2 & 1 & 0 & 0 & 0 \\ 0 & 1 & 2 & 1 & 0 & 0 \\ . & . & . & . & . & . \\ . & . & . & . & . & . \\ 0 & 0 & 0 & -1 & 2 & 1 \end{bmatrix} \quad (21)$$

$$B=\begin{bmatrix} -1 & 3 & -3 & 1 & 0 & 0 & 0 \\ 0 & -1 & 3 & -3 & 1 & 0 & 0 \\ . & . & . & . & . & . & . \\ . & . & . & . & . & . & . \\ . & . & . & . & . & . & . \\ 0 & 0 & 0 & -1 & 3 & -3 & 1 \end{bmatrix} \quad (22)$$

In this study, the first order regularization is employed. Matrix R is also defined as follows:

$$\begin{bmatrix} \Delta r_1 & 0 & . & . & 0 \\ \Delta r_1 & \Delta r_2 & . & . & 0 \\ . & . & . & . & . \\ . & . & . & . & . \\ \Delta r_1 & \Delta r_2 & . & . & \Delta r_N \end{bmatrix} \quad (23)$$

Moreover, elements of matrix R, according to the Laplace equation are:

$$\Delta r_i=\frac{[r_k p(i-1)-r_k p(i)]}{M(P_i)} \quad (24)$$

where:

$$r_k p(i)=\frac{2\sigma\cos\theta}{p(i)} \quad (25)$$

Matrix Q is obtained from the experimental data. So, the equation can be written as follows:

$$\begin{bmatrix} \Delta r_1 & 0 & . & . & 0 \\ \Delta r_1 & \Delta r_2 & . & . & 0 \\ . & . & . & . & . \\ . & . & . & . & . \\ \Delta r_1 & \Delta r_2 & . & . & \Delta r_N \end{bmatrix} \begin{bmatrix} f_1(r) \\ f_2(r) \\ . \\ . \\ Q_N \end{bmatrix} = \begin{bmatrix} Q_1 \\ Q_2 \\ . \\ . \\ Q_N \end{bmatrix} \quad (26)$$

The optimal level of regularization parameter (λ) should be selected to establish the best stabilization of the solution vector $f(r)$. Various criteria (e.g. LOOCV, LC, UC and MLC) have been used in literatures for selection of optimum regularization parameter (λ). In this study, we have used the Leave One Out Cross Validation (LOOCV) method [38].

$$CV(\lambda)=\frac{1}{N}\sum_{k=1}^{N}[\frac{\underline{e}_k^T[I_N-H(\lambda)]\underline{y}}{\underline{e}_k^T[I_N-H(\lambda)]\underline{e}_k^T}]^2 \quad (27)$$

where:

$$H(\lambda)=R(R^TR+\lambda B^TB)^{-1}R^T \quad (28)$$

The optimal value of regularization parameter can be selected by minimization of the above merit function. For this purpose, we need to calculate the inverse of matrix $M\times M(R^TR+\lambda B^TB)$.

3. CASE STUDIES

3. 1. Case Study No. 1 In this case study, the data of CFP method on 10 μm-thickness polycarbonate track-etched membrane (T-3) are examined. Other related information for this case was obtained from literature [21]. The Porometerused in this test can be governed in the range of 0-30 barstandard pressure with flux above 200 1/min. Liquid used for this test (coulter porofil) had low surface tension (γ=16×10-3 N/M), low vapor pressure (3 mmHgat 298 K), and low reactivity which can be assumed the contact angle for all pores is zero ($\theta=0^\circ$). The gas used in this experiment was air. To measure the CFP, the membrane sample has been immersed and wetted in the liquid for 1 h at room temperature. An example of the directly measured wet flow-state for the track-etched polycarbonate membranes (T-3) is shown in Figure 5.

3. 2. Case Sstudy No. 2 The data of polycarbonate membrane bubble point (C04) with 0.4 μm pore diameter, 10 μm thickness, and 13% mean porosity has been examined in this case [39]. The liquid used for the bubble test experiment (coulter porofil) had a low surface tension (γ=16×10-3N/M), low vapor pressure (3 mmHg at 298 K), and low reactivity. Therefore, it was assumed the contact angle for all pores is zero ($\theta=0^\circ$). An example of the directly measured wet flow-state is shown in Figure 6 for this C04 membrane.

3. 3. Case Study No. 3 In this case, the data of polycarbonate membrane bubble point (N08) with 0.8 μm pore diameter, 9 μm thickness, and 15% mean porosity has been examined. Other information related to this case was obtained from reference [40]. The bubble point pressure of the membrane is at least 1.24× 10^5 Pa for water. Also, it has a regular porous medium with cylindrical pores and uniform size. The membrane has been used for the bubble point method with liquid replacement technique. The liquid used for this experiment (coulter porofil) had a low surface tension (γ=16×10-3 N/M), low vapor pressure (3 mmHg at 298

K) and low reactivity. It could be assumed that the contact angle for all pores is zero ($\theta=0^{\circ}$). The gas used in the experiment was air. An example of the directly measured wet floe-state is shown in Figure 7 for the N08 membrane.

3. 4. Case Study No. 4 For the second case, the bubble point test data of a symmetric integrated membrane of mixed cellulose ester (MCE) has been studied [41]. In the gas-liquid concentration test, high purity nitrogen gas, n-butanol (γ=24.5 dyns/cm) and deionizer water (γ=72 dyns/cm) as wetter liquid have been used. Therefore, it was assumed the contact angle for all pores is zero ($\theta=0^{\circ}$). An example of the directly measured wet flow-state for MCE membrane is shown in Figure 8. Table 1 provides a summary of information of the membranes and bubble point test for four different case studies.

4. RESULTS AND DISCUSSION

To evaluate the validity and accuracy of this approach, the PSD obtained from the proposed method in this study were compared with the PSD data presented in the literatures. In the case study 1, the CFP experiment has shown that the PSD of membrane has two sharp peaks at about 256 nm and 320 nm and also, there are very few pores smaller than 200 nm (Figure 9). Figure 9 also shows PSD of the membrane obtained according to SEM images. SEM results show that the membrane has two peaks around 226 nm and 320 nm. In addition, according to only wet flow-state data, the PSD of membrane using the proposed method is shown in Figure 9. The results indicate two peaks at 254 nm and 320 nm. By comparing the results of the proposed method with those of CFP and SEM, we can conclude that the proposed method is reasonably accurate.

In the case study 2, mean pore diameter calculated from the air porometry method is $0.462\mu m$. Moreover, mean pore diameter calculated from the mercury porometry method is $0.401\mu m$. Finally, the PSD obtained using the proposed method is shown in Figure 10. By comparing the mean pore size calculated by the proposed method which is about $0.4614\mu m$, with those reported in the literature [39], the accuracy of the proposed method is confirmed.

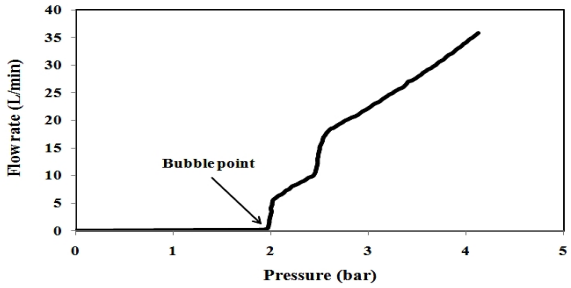

Figure 5. Wet flow-state of the porometer for the track-etched membranes (T-3) [21].

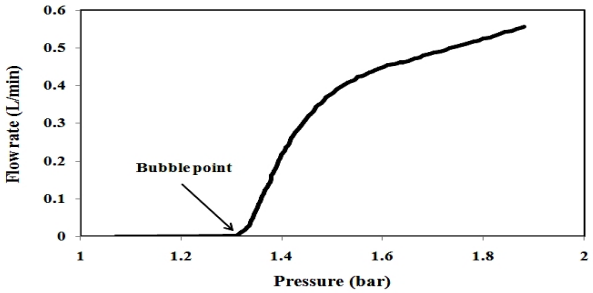

Figure 6. Wet flow-state of the porometer for C04 membranes [39].

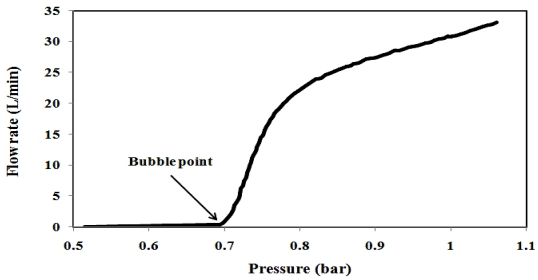

Figure 7. Wet flow-state of the porometer for N08 membranes [40]

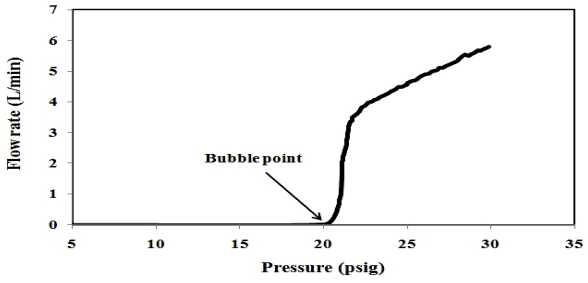

Figure 8. Wet flow-state of the porometer for MCE membranes [41].

TABLE 1. Summary information of case studies.

NO.	Membrane	Gas (A)	Liquid (B)	σ (N/m)	θ (°)	Thickness (µm)	Porosity (%)	Ref.
1	T-3	Air	coulter porofil	0.016	0	10	-	[21]
2	C04	Air	coulter porofil	0.016	0	10	13	[39]
3	N08	Air	coulter porofil	0.016	0	9	15	[40]
4	MCE	N_2	n-butanol & H_20	0.072 & 0.0245	0	-	-	[41]

In the case study 3, mean pore diameter calculated from the air porometry method is $0.86 \pm 0.04 \mu m$. By comparing the PSD calculated by the proposed method (about $0.835 \mu m$, shown in Figure 11) with those reported in the literature [40], we can confirm the accuracy of the proposed method. In the case study 4, according to the data obtained from the wet flow-state (Figure 8) as well as the liquid used in the gas–liquid porometry test, the PSD of MCE membrane is calculated by the proposed method (Figure 12). Mean pore diameter of the MCE membrane calculated by the proposed method is about $0.555 \mu m$ which is roughly consistent with the mean pore diameter reported in the literature ($0.55 \mu m$) [41]. The optimal λ parameters chosen by LOOCV method for each case study are shown in Table 2. Table 3 provides a comparison between the results obtained by different methods and the proposed method in this study to calculate the average diameter of the membranes. By comparing the results obtained from different procedures, the accuracy of the proposed method is confirmed. Also, considering this method in which the number of discretization in each interval (M(P)) is adjustable, the number of output points (f(r) and r) can be much greater than the number of input points (P and Q). Even with a very low number of input points (from wet flow-state), the NPSD of membranes (a curve without fracture) can be obtained. For example, if input data are reduced to four points for case 4, according to previous techniques, only 3 points of f(r) and r can be achieved (because wet flow-state diagram has three slope) and appropriate curve for NPSD cannot be achieved. According to proposed method in this study, with 4 input data in case 4, if M(P)=2, the eight output data was calculated (minimum number of output data for 4 input data). The NPSD of this membrane is shown in Figure 13.

TABLE 2. Optimal λ parameters.

Case study	1	2	3	4
Optimum λ	10^{-10}	10^{-22}	10^{-16}	10^{-25}

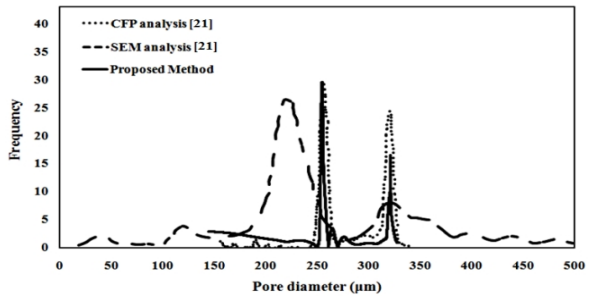

Figure 9. Pore diameter distribution of T-3 membrane obtained from CFP analysis [21], analysis of SEM images [21] and proposed method.

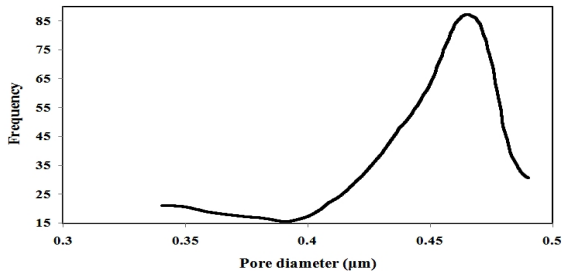

Figure 10. Pore diameter distribution of C04 membrane obtained from the proposed method.

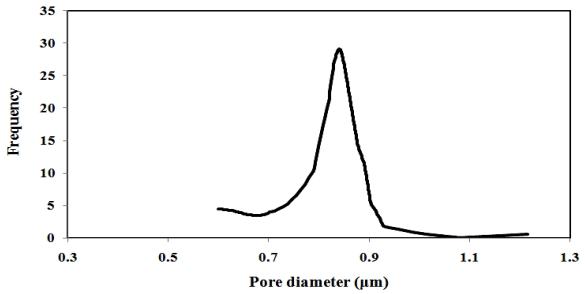

Figure 11. Pore diameter distribution of N08 membrane obtained from the proposed method.

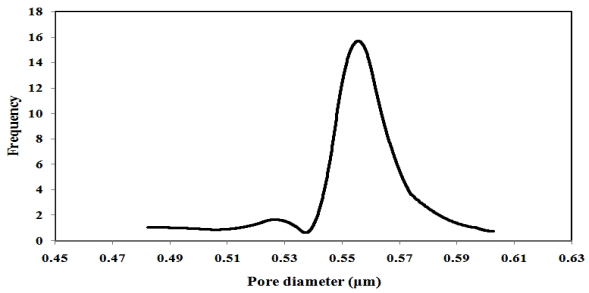

Figure 12. Pore diameter distribution of MCE membrane obtained from the proposed method.

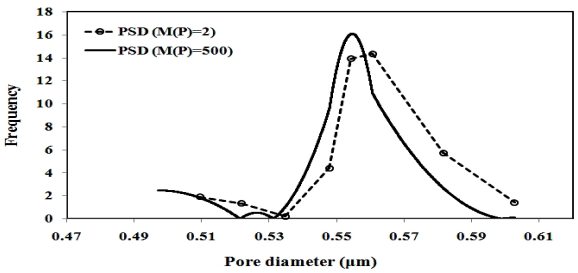

Figure 13. Pore diameter distribution of MCE membrane obtained from the proposed method by M(P)=2 and M(P)=500.

As shown in the figure, even with 8 output data, good diagram of NPSD cannot be achieved. Usually at this situation, a Gaussian function fitting is used. This procedure will cause a large error. For case 4, if M(P)=500, via 4 obtained data from the wet flow-state diagram (input data), 2000 output data points can be calculated, then the NPSD diagram of this membrane

TABLE 3. Comparison between the results obtained by the different methods and the proposed method.

NO.	M[1]	PM[2] (μm)	AP[3] (μm)	MP[4] (μm)	SEM (μm)	Ref.
1	T-3	0.32& 0.254	0.32& 0.256	-	0.32&0.226	[21]
2	C04	0.4614	0.462	0.401	-	[39]
3	N08	0.835	0.86 ± 0.04	-	0.69 ± 0.04	[40]
4	MCE	0.555	0.55	-	-	[41]

[1]Membrane Type[3]Air Porometer
[2]Proposed Method[4]Mercury Porometer

will be obtained without fracture (Figure 13) and fitting by a Gaussian function is not required. According to obtained results, Figure 12 (which is calculated with high input data) is clearly similar to the Figure 13 (continues line).

5. CONCLUSION

In this study, the determination of the neck-pore size distribution has been examined by using the wet flow-state bubble point test data. The first order linear regularization method has been used in order to dissolve the integral equation governing the process, which the optimized λ parameter acquired from LOOCV method. In this study, there are different case studies of various literatures that each one used for obtaining of many membrane pores determined by acquiring the wet flow curve and data related to the bubble point experiments.

The comparison between the results made by different methods and proposed method in this study has showed the accuracy in this theory clearly, in order to determine the neck-pore size distribution of membranes. The main features of the proposed method can be summarized: (1) No need to the dry flow-state data (Q_d). (2) Does not require priori information about the flux of fluid A coming out of the pore which its size equals to r ($G(r)$) and unlike the forward method, it provides an optimal solution for the NPSD. (3) Have an answer in $P > P_{\max}$ and $P < P_{\min}$ and smooth curve. (4) In this method, the number of discretization in each interval is adjustable and the number of output points can be much greater than the number of input points. (5) Unlike traditional methods, even with a very low number of input points (from wet flow-state), it can be found NPSD of membranes (a curve without fracture). According to the results, this method can be replaced for existent multi-step method appropriately. In other words, this is practically the only available method to calculate the NPSD of membranes by using the minimum number of experimental and physical data (only need to wet flow-state and no need to $G(r)$ function) and offers a significant performance in obtaining of the NPSD of porous membranes.

6. REFERENCES

1. Sahimi, M. and Tsotsis, T.T., "Molecular pore network models of nanoporous materials", ***Physica B: Condensed Matter***, Vol. 338, No. 1, (2003), 291-297.
2. Steriotis, T., Mitropoulos, A., Kanellopoulos, N., Keiderling, U. and Wiedenmann, A., "Characterization of an alumina membrane by neutron scattering and other techniques", ***Physica B: Condensed Matter***, Vol. 234, No., (1997), 1016-1018.
3. Fang, Y., Bian, L., Bi, Q., Li, Q. and Wang, X., "Evaluation of the pore size distribution of a forward osmosis membrane in three different ways", ***Journal of Membrane Science***, Vol. 454, No., (2014), 390-397.
4. Bechhold, H., Schlesinger, M., Silbereisen, K., Maier, L. and Nurnberger, W., "Pore diameters of ultrafilters", ***Kolloid Z***, Vol. 55, (1931), 172-198.
5. Carretero, P., Molina, S., Lozano, A., de Abajo, J., Calvo, J.I., Prádanos, P., Palacio, L. and Hernández, A., "Liquid–liquid displacement porosimetry applied to several mf and uf membranes", ***Desalination***, Vol. 327, (2013), 14-23.
6. Antón, E., Calvo, J.I., Álvarez, J.R., Hernández, A. and Luque, S., "Fitting approach to liquid–liquid displacement porosimetry based on the log-normal pore size distribution", ***Journal of Membrane Science***, Vol. 470, (2014), 219-228.
7. Honold, E. and Skau, E.L., "Application of mercury-intrusion method for determination of pore-size distribution to membrane filters", ***Science***, Vol. 120, No. 3124, (1954), 805-806.
8. Stefanopoulos, K., Steriotis, T.A., Mitropoulos, A.C., Kanellopoulos, N. and Treimer, W., "Characterisation of porous materials by combining mercury porosimetry and scattering techniques", ***Physica B: Condensed Matter***, Vol. 350, No. 1, (2004), E525-E527.
9. Riedel, C. and Spohr, R., "Transmission properties of nuclear track filters", ***Journal of Membrane Science***, Vol. 7, No. 2, (1980), 225-234.
10. Clarke, D., "Review: Transmission scanning electron microscopy", ***Journal of Materials Science***, Vol. 8, No. 2, (1973), 279-285.
11. Binnig, G., Quate, C.F. and Gerber, C., "Atomic force microscope", ***Physical review letters***, Vol. 56, No. 9, (1986).
12. Meyer, E., "Atomic force microscopy", ***Progress in surface science***, Vol. 41, No. 1, (1992), 3-49.
13. Sarbolouki, M., "A general diagram for estimating pore size of ultrafiltration and reverse osmosis membranes", ***Separation Science and Technology***, Vol. 17, No. 2, (1982), 381-386.
14. Dollimore, D. and Heal, G., "An improved method for the calculation of pore size distribution from adsorption data", ***Journal of Applied Chemistry***, Vol. 14, No. 3, (1964), 109-114.
15. Lloyd, D.R., "Materials science of synthetic membranes", (1985).
16. Brun, M., Lallemand, A., Quinson, J.-F. and Eyraud, C., "A new method for the simultaneous determination of the size and shape of pores: The thermoporometry", ***Thermochimica acta***, Vol. 21, No. 1, (1977), 59-88.
17. Mey-Marom, A. and Katz, M., "Measurement of active pore size distribution of microporous membranes-a new approach", ***Journal of Membrane Science***, Vol. 27, No. 2, (1986), 119-130.
18. Cuperus, F., Bargeman, D. and Smolders, C., "Permporometry: The determination of the size distribution of active pores in uf membranes", ***Journal of Membrane Science***, Vol. 71, No. 1, (1992), 57-67.
19. Glaves, C.L. and Smith, D.M., "Membrane pore structure analysis via nmr spinlattice relaxation experiments", ***Journal of Membrane Science***, Vol. 46, No. 2, (1989), 167-184.

20. Hassan, J., "Pore size distribution calculation from 1 h nmr signal and n 2 adsorption–desorption techniques", ***Physica B: Condensed Matter***, Vol. 407, No. 18, (2012), 3797-3801.
21. Agarwal, C., Pandey, A.K., Das, S., Sharma, M.K., Pattyn, D., Ares, P. and Goswami, A., "Neck-size distributions of through-pores in polymer membranes", ***Journal of Membrane Science***, Vol. 415, No., (2012), 608-615.
22. Fang, Y., Tolley, H.D. and Lee, M.L., "Simple capillary flow porometer for characterization of capillary columns containing packed and monolithic beds", ***Journal of Chromatography A***, Vol. 1217, No. 41, (2010), 6405-6412.
23. Piątkiewicz, W., Rosiński, S., Lewińska, D., Bukowski, J. and Judycki, W., "Determination of pore size distribution in hollow fibre membranes", ***Journal of Membrane Science***, Vol. 153, No. 1, (1999), 91-102.
24. Morozov, V.A., Nashed, Z. and Aries, A., "Methods for solving incorrectly posed problems, Springer New York, (1984).
25. Phillips, D.L., "A technique for the numerical solution of certain integral equations of the first kind", ***Journal of the ACM (JACM)***, Vol. 9, No. 1, (1962), 84-97.
26. Tikhonov, A.N., Arsenin, V.I.A.k. and John, F., "Solutions of ill-posed problems, Winston Washington, DC, (1977).
27. Press, W.H., Teukolsky, S.A., Vetterling, W.T. and Flannery, B.P., *Numerical recipes in fortran (cambridge*. 1992, Cambridge Univ. Press.
28. Shahsavand, A. and Shahrak, M.N., "Direct pore size distribution estimation of heterogeneous nano-structured solid adsorbents from condensation data: Condensation with no prior adsorption", ***Colloids and Surfaces A: Physicochemical and Engineering Aspects***, Vol. 378, No. 1, (2011), 1-13.
29. Press, W.H., Vetterling, W.T., Teukolsky, S.A., Flannery, B.P. and Greenwell Yanik, E., "Numerical recipes in fortran--the art of scientific computing", ***SIAM Review***, Vol. 36, No. 1, (1994), 149-149.
30. Ahmadian, H., Mottershead, J. and Friswell, M., "Regularisation methods for finite element model updating", ***Mechanical Systems and Signal Processing***, Vol. 12, No. 1, (1998), 47-64.
31. Krakauer, N.Y., Schneider, T., Randerson, J.T. and Olsen, S.C., "Using generalized cross-validation to select parameters in inversions for regional carbon fluxes", ***Geophysical research letters***, Vol. 31, No. 19, (2004).
32. Yagola, A. and Titarenko, V., "Numerical methods and regularization techniques for the solution of ill-posed problems", in Inverse Problems in Engineering: Theory and Practice. Vol. 1, (2002), 49-58.
33. Yeun, Y.S., Lee, K.H., Han, S.M. and Yang, Y.S., "Smooth fitting with a method for determining the regularization parameter under the genetic programming algorithm", ***Information Sciences***, Vol. 133, No. 3, (2001), 175-194.
34. Luo, J. and Li, X., "An inverse aeroacoustic problem on rotor wake/stator interaction", ***Journal of sound and vibration***, Vol. 254, No. 2, (2002), 219-229.
35. Venkatesh, P.K., "On tikhonov regularisation", ***Physica A: Statistical Mechanics and its Applications***, Vol. 284, No. 1, (2000), 448-460.
36. Hansen, O., Fischer, S. and Ramlau, R., "Regularization of mellin-type inverse problems with an application to oil engineering", ***Linear algebra and its applications***, Vol. 391, (2004), 125-147.
37. Lamm, P.K., "Variable-smoothing regularization methods for inverse problems", (1999).
38. Golub, G.H. and Van Loan, C.F., "Matrix computations, JHU Press, Vol. 3, (2012).
39. Hernández, A., Calvo, J., Prádanos, P. and Tejerina, F., "Pore size distributions in microporous membranes. A critical analysis of the bubble point extended method", ***Journal of Membrane Science***, Vol. 112, No. 1, (1996), 1-12.
40. Hernandez, A., Calvo, J., Pradanos, P. and Tejerina, F., "Pore size distributions of track-etched membranes; comparison of surface and bulk porosities", ***Colloids and Surfaces A: Physicochemical and Engineering Aspects***, Vol. 138, No. 2, (1998), 391-401.
41. Shrestha, A., Pellegrino, J., Husson, S.M. and Wickramasinghe, S.R., "A modified porometry approach towards characterization of mf membranes", ***Journal of Membrane Science***, Vol. 421, No., (2012), 145-153.

A New Approach for Determination of Neck-Pore Size Distribution of Porous Membranes via Bubble Point Data

M. Arjmandi[a], O. Pirouzram[b], A. Ahmadpour[a]

[a] *Department of Chemical Engineering, Faculty of Engineering, Ferdowsi University of Mashhad, Mashhad, Iran*
[b] *Department of Chemical Engineering, Faculty of Engineering, Kurdistan University, Kurdistan, Iran*

PAPER INFO

Paper history:
Received 19 July 2014
Received in revised form 12 March 2014
Accepted 30 April 2015

Keywords:
Membrane
NPSD
Regularization
Cross-Validation

چکید

تخمین قابل اعتماد توزیع سایز گردنه غشاها عنصر اصلی در طراحی و عملکرد همه فرایندهای جداسازی غشایی است. در این مقاله، یک رویکرد جدید برای تعیین قابل اعتماد توزیع اندازه گردنه حفرات غشاهای متخلخل با استفاده از داده‌های آزمایشگاهی حالت جریان تر ارائه داده شده است. برای این منظور، یک روش قدرتمند بر پایه تئوری ریگولاریزاسیون خطی برای به دست آوردن توزیع اندازه گردنه حفرات غشاها به کمک داده‌های آزمایش نقطه حباب گسترش داده شده است. کارایی این روش ارائه شده با استفاده از داده های آزمایشگاهی مختلف مورد آزمایش قرار گرفته است. نتایج پیش بینی شده به طور واضح نشان می دهد که این روش پیشنهادی به طور موفقیت آمیز می تواند توزیع اندازه منافذ قابل قبولی به کمک مجموعه ای از داده های آزمایش نقطه حباب پیش بینی کند.

***doi**: 10.5829/idosi.ije.2015.28.06c.01*